Journal of Structural Geology 32 (2010) 1488–1499

Contents lists available at ScienceDirect

Journal of Structural Geology

journal homepage: www.elsevier.com/locate/jsg

Tabular fracture clusters: Dynamic fracturing produced by volatile expulsion, Sierra Nevada Batholith, California

P. Riley*, B. Tikoff

University of Wisconsin-Madison, 1215 W. Dayton St., Madison, WI 53706, USA

ARTICLE INFO

Article history:
Received 14 April 2010
Received in revised form
1 September 2010
Accepted 18 September 2010
Available online 25 September 2010

Keywords:
Tuolumne intrusive suite
Dynamic fracturing
Volatile expulsion
Fracture
Sierra Nevada batholith

ABSTRACT

An undocumented type of fracture system – Tabular Fracture Clusters (TFCs) – occurs in the Cathedral Peak granodiorite, Sierra Nevada Batholith, CA. TFCs are linear zones of sub-parallel, densely spaced fractures, approximately 4–40 cm wide and 3–100 m long. TFCs occur in highest density adjacent to the Johnson granite porphyry, which intruded the Cathedral Peak granodiorite. Individual fractures in TFCs exhibit only opening-mode displacement. Microstructural analysis indicates that TFC fractures contain micro-breccia of angular clasts of host rock. Fine-grained zeolite and quartz are observed along many of the fractures within TFCs, all of which are absent in the host rock. The characteristics of TFCs suggest that they differ from previously documented fracture systems in the Sierra Nevada Batholith. The dense spacing, nature of the fractures, and association of TFCs with miarolitic cavities provide compelling evidence that TFCs formed in response to volatile overpressure from the adjacent Johnson granite porphyry. We attribute the formation of TFCs to dynamic fracturing, based on the clustered nature of the extension fractures and the geometric similarities of TFCs to other dynamic fracturing arrays.

1. Introduction

The process of fracturing results in numerous fracture types that organize in different manners. Within fracture sets, shear fractures –fractures with observable shear displacement – are commonly clustered (e.g., Mitra, 1984; Little, 1996; Watterson et al., 1996), but extension fractures – fractures that display only opening-mode displacement – are generally anti-clustered. This difference is attributed to the stress reduction shadow produced once a single extension fracture has formed (e.g., Price, 1966; Hobbs, 1967; Gross, 1993).

Clusters of extensional fractures are often attributed to heterogeneities (terminations, step-overs) produced by shear fractures and faults (e.g., Cruikshank and Aydin, 1995; Myers and Aydin, 2004). In the absence of shearing, experimental evidence suggests extensional fracture clusters can form due to high strain rates (2×10^{-3} s^{-1} to 7×10^{-3} s^{-1}) through dynamic fracturing (Sagy et al., 2001; Griffith et al., 2009). Numerous experimental examples of dynamic fracturing exist (Sharon and Fineberg, 1996; Sagy et al., 2001; Griffith et al., 2009), but field examples are presently limited to shatter cones (Sagy et al., 2002, 2004) and pseudotachylyte injection from earthquake rupture (Di Toro et al., 2005).

In this study, we describe a fracture system in the Cathedral Peak granodiorite, Sierra Nevada Batholith. This fracture system consists of cm-m wide clusters of densely spaced, sub-parallel, extension fractures, which we term Tabular Fracture Clusters (TFCs). On a regional scale: most TFCs form in a single orientation, but locally two orthogonal sets are developed; and TFCs are spatially associated with the exposed and sub-surface extent of the Johnson granite porphyry. Strain estimates from TFC arrays record elongation perpendicular (0.5–4.5%) and occasionally parallel (0.4–2.1%) to the long axis of the Johnson granite porphyry. We propose that TFCs are a result of dynamic fracturing, formed by the rapid release of overpressured volatiles, evidenced by a series of fluid-rich magmatic features associated with these structures. The intrusion of the Johnson granite porphyry provides the source of the volatiles, the rapid strain rates necessary for dynamic fracturing, and explains the array of TFC orientations.

2. Geologic setting

The Tuolumne Intrusive Suite (Fig. 1), situated in the east-central Sierra Nevada Batholith, is a well-known example of a nested plutonic complex, consisting of a series of plutons that young and become increasingly felsic towards the intrusive suite

* Corresponding author. Tel.: +1 608 262 8960; fax: +1 608 262 0693.
E-mail address: priley@geology.wisc.edu (P. Riley).

0191-8141/$ – see front matter © 2010 Elsevier Ltd. All rights reserved.
doi:10.1016/j.jsg.2010.09.006

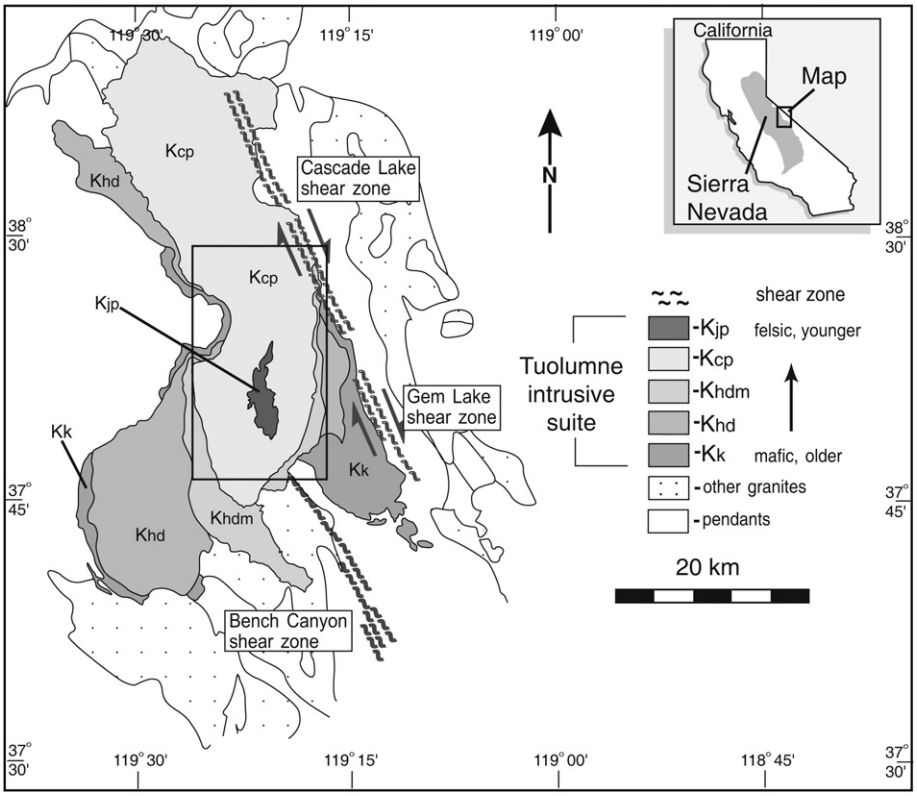

Fig. 1. Tuolumne Intrusive Suite and surrounding rocks. Box indicates location of Fig. 6. Khd-Half Dome granodiorite; Kjp-Johnson granite porphyry; Kcp- Cathedral Peak granodiorite; Khdm- Half Dome granodiorite megacrystic; Kk- Kuna Crest granodiorite. Modified from Bateman and Chappell (1979), Tikoff and Saint Blanquat (1997), and Titus et al. (2005).

center (Bateman, 1992). From the outermost (oldest) plutons inward, the intrusive suite consists of the Kuna Crest granodiorite (93.5 ± 0.7 Ma), the Glen Aulin tonalite (93.1 ± 0.1 Ma), the Half Dome granodiorite (92.8 ± 0.2 Ma at its exterior to 88.8 ± 0.8 Ma at its interior), the Cathedral Peak granodiorite (88.1 ± 0.2 Ma), and the Johnson granite porphyry (85.4 ± 0.1 Ma) (Coleman et al., 2004). The older plutons at the margins are predominantly granodiorite (total percent K-feldspar <20%), and progressively grade to granite in the younger plutons (total percent K-feldspar >30%).

This study focuses on the two innermost plutons, the Cathedral Peak granodiorite and the Johnson granite porphyry. The Cathedral Peak granodiorite is porphyritic, containing large (4–5 cm) K-feldspar megacrysts. Megacrysts are most abundant near the contact with the Half Dome granodiorite, and decrease in both size and abundance towards its interior (Bateman and Chappell, 1979). Despite the variations in megacryst size and abundance, the percent K_2O is constant across the pluton, with megacrysts forming at the expense of smaller K-feldspar grains. The groundmass is similar in composition to the Half Dome granodiorite, but mafic phases are smaller and less noticeable. With increasing proximity to the Johnson granite porphyry at its interior, an increase in aplite dikes occurs in the Cathedral Peak granodiorite. Aplite dikes can be traced from the Johnson granite porphyry into the Cathedral Peak granodiorite, and are thus thought to be a product of Johnson granite porphyry intrusion (Bateman, 1992; Titus et al., 2005).

The Johnson granite porphyry, a fine-grained leucogranite, is the youngest pluton in the Tuolumne Intrusive Suite, emplaced at 85.4 ± 0.1 Ma (Coleman and Glazner, 1997). Mafic phases are almost non-existent. Xenoliths of the Cathedral Peak granodiorite, ranging in size from cm to 100s-m, are abundant and display both sharp and gradational contacts (Titus et al., 2005). Miarolitic cavities, aplite dikes, and pegmatite veins are abundant throughout the Johnson granite porphyry. The fine-grained nature and the presence of miarolitic cavities led to the inference that the Johnson granite porphyry was a 'quenched' pluton, with abundant fluids (Bateman, 1992). Bateman (1992) suggested that a decrease in pressure could lead to quenching, possibly due to a volcanic eruption.

The Tuolumne Intrusive Suite was emplaced at shallow crustal levels (1–3 kbar or ~3–10 km depth; Ague and Brimhall, 1988) during active tectonism in the Sierra Nevada magmatic arc. During intrusion of the Tuolumne Intrusive Suite, the Sierra Nevada Batholith experienced dextral transpression, causing the formation of numerous shear zones, collectively termed the Sierra Crest shear zone system (e.g., Tikoff and de Saint Blanquat, 1997). Dextral shear zones affect the eastern edge of the Tuolumne Intrusive Suite in the CascadeLake (Tikoff et al., 2005) and Gem Lake shear zones (Greene and Schweickert, 1995). At its southern margin, the dextral Bench Canyon shear zone in the Ritter Range roof pendant is truncated by the intrusive suite, but may have influenced intrusive suite shape and emplacement (McNulty, 1995; Titus et al., 2005).

3. Tabular fracture clusters (TFCs)

Fracture sets in the Sierra Nevada Batholith have received attention dating back to Mayo (1941). Large-scale systematic fracture sets, formed in the Late Cretaceous (Segall et al., 1990), were documented via aerial photographs by Lockwood and Lydon (1975) and Lockwood and Moore (1979). More recent studies of the Late Cretaceous lineaments have been focused in the southern section (i.e, south of 37°15′N. lat.) of the batholith (e.g., Segall and Pollard, 1983a, 1983b; Segall et al., 1990; Bergbauer and Martel, 1999; Pachell and Evans, 2002; Pachell et al., 2003; d'Alessio and Martel, 2005). The fractures in this study are variably spaced,

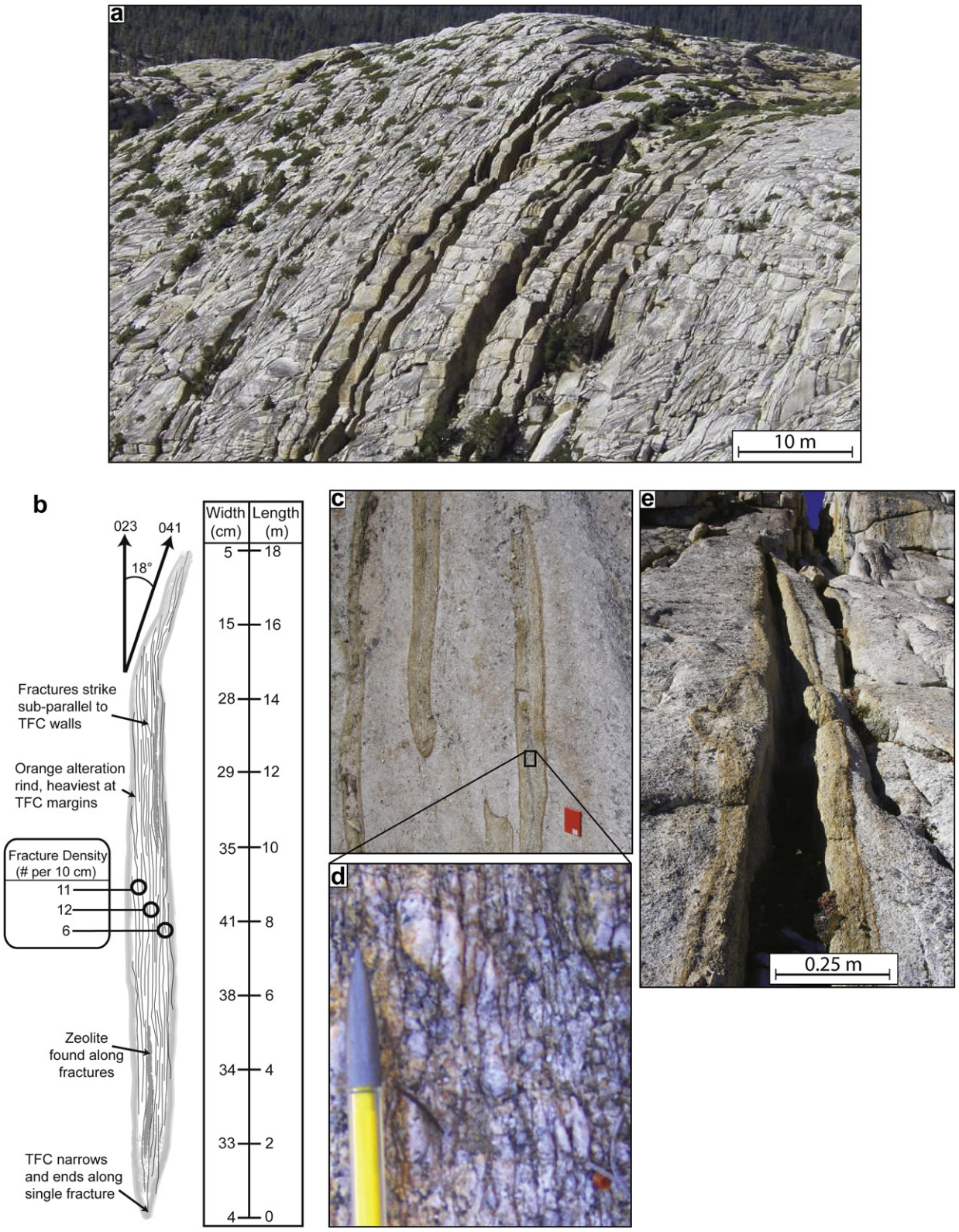

Fig. 2. a) Large-scale view of a swarm of TFCs near Budd Lake. Large gullies are due to erosion of multiple, closely spaced TFCs. b) Schematic drawing of a measured TFC illustrating key characteristics. c) Field photograph of TFCs with field book for scale. Note their sub-parallel nature and orange alteration rind. d) Close up of fracturing within TFC shown in (c). Macroscopic fracturing is sub-parallel to the overall TFC, with no observable shear offset. e) Field photograph illustrating weathering characteristics of TFCs.

ranging from 10s of cm-scale spacing up to 10s of m-scale spacing, and are commonly associated with a bleached zone and mineralization along the fracture plane (Segall and Pollard, 1983a; Segall et al., 1990). Studies on these fracture sets have yielded insight into jointing in cooling plutons (Bergbauer and Martel, 1999), shear fracture initiation (Segall and Pollard, 1983b; d'Alessio and Martel, 2005), deformation and stress associated with joints (Segall and Pollard, 1983a), and large-scale kink band evolution (Pachell

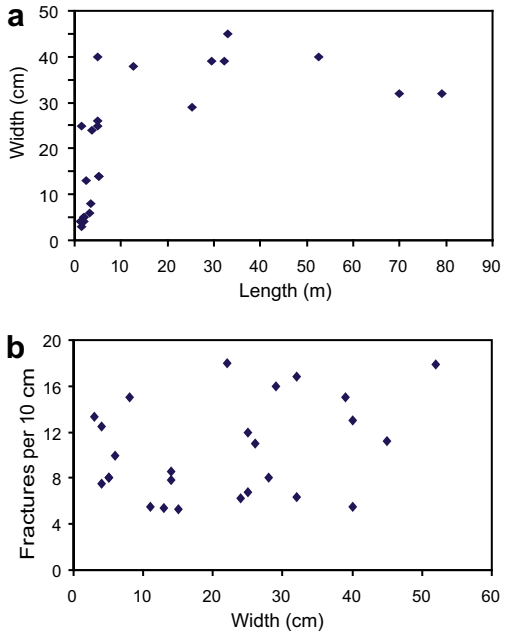

Fig. 3. a) TFC length vs. width. TFC width increases with increasing length for TFCs <7 m, but is constant for TFCs >7 m in length. b) TFC width vs. number of fractures per 10 cm. No correlation exists between fracture density and width.

et al., 2003). We report on a fracture system – tabular fracture clusters – developed in the Cathedral Peak granodiorite that do not fit in any of these previous studies.

3.1. Field characterization

Tabular Fracture Clusters (TFCs) are tabular zones of densely spaced fractures that occur in clustered sets within the Cathedral Peak granodiorite (Fig. 2a–e). Fracture density is always ≥4 fractures per 10 cm (fracture density hereafter referred to as # per 10 cm), an empirical criterion derived in the field. The margins of the TFC display an abrupt (<5 cm) change from essentially unfractured rock to the dense fracturing. Within each TFC, the lowest fracture densities are observed at TFC margins, and the maximum fracture densities are observed in the center, although fracture density is always ≥4 per 10 cm regardless of the measurement location. Individual TFC fractures are sub-parallel to the walls of the zone and are 10–100 cm long (Fig. 2c,e). Where fracture faces can be observed, no striations, plumose structures, or other structures are observed. Fractures are curvi-planar, undulating ±5° from the overall strike of the TFC.

Maximum TFC width, measured at the widest part of a TFC perpendicular to its strike, mostly range from 0.04 to 0.40 m (Fig. 3a). Width is variable along strike, with the widest part of a TFC typically occurring at its along strike mid-point and narrowing towards the tips (terminations). TFC length is measured parallel to TFC strike from tip to tip, with the TFC tip marked by the ending of the last fracture clearly occurring within the continuous zone of TFC fractures. TFC length ranges from 3 to 100 m (Fig. 3a). Maximum TFC width increases linearly with increasing length for TFCs <7 m long, but remains constant at ~40 cm for TFCs longer than 7 m (Fig. 3a). Fracture densities range from 5 per 10 cm up to 18 per 10 cm, and show no systematic variation with width (Figs. 3b and 4a).

The tips of TFCs exhibit several characteristics that distinguish them from the main part of a TFC. First, at least one TFC tip, if not both, deviates from the overall strike of the main TFC by ~15°, with no systematic clockwise or counter-clockwise deviation. Fig. 2a shows the characteristics of a measured TFC that is 18 m long, in which a change in strike occurs in the last 3 m (Fig. 2a). Second, the amount of fracturing also decreases towards TFC tips. For example, a TFC with many (>50) fractures in its central portion may only have 4–5 at its tip, with the TFC ending along a single fracture that extends slightly farther than the rest.

An orange alteration rind is often associated with TFC edges (Fig. 2a,b,d,e), occurring in >90% of observed TFCs. It is

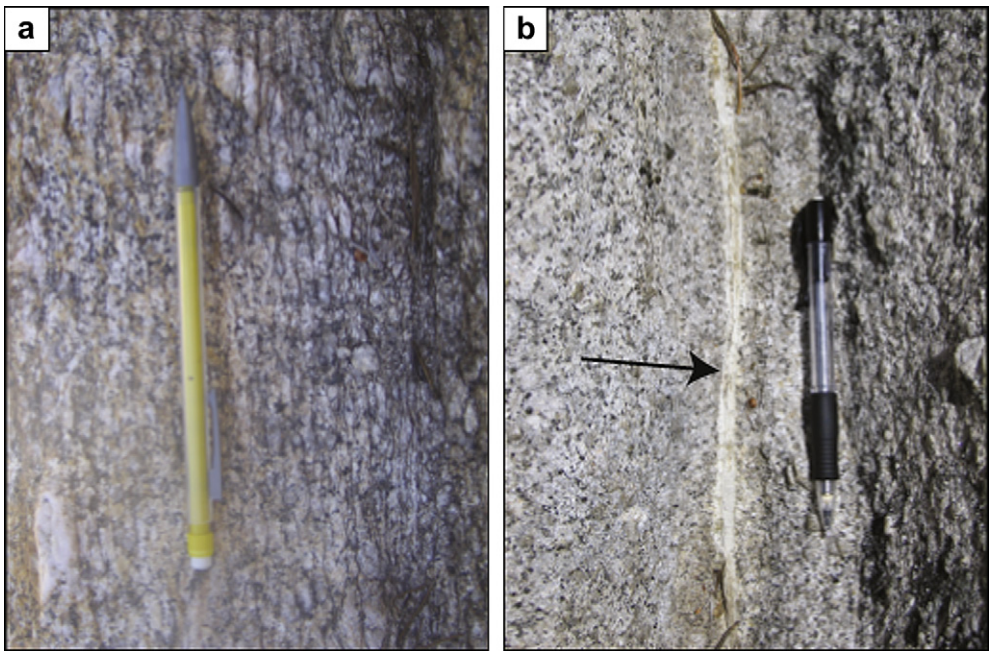

Fig. 4. a) Field photograph illustrating the dense fracturing observed within a TFC. Note the sub-parallel nature of the fractures. b) Field photograph illustrating white, fine-grained material (arrow) identified as zeolite/quartz mixture found at every field locality within at least one TFC.

concentrated outside of the dense fracturing as 5–10 cm wide swaths parallel to the strike of the TFC, with minor orange coloration within the TFCs. Where TFCs of different orientations interact, the orange alteration rind forms a continuous envelope around the structures (Fig. 2a,b,d,e).

TFCs are commonly associated with zones of increased erosion, informally called gullies, parallel to the strike of the TFC (Fig. 2a,e). The width of a gully is typically larger than the TFC within it. Larger TFC-bounded gullies are up to 2–3 m wide, but the bottoms of these gullies typically are covered by sediment and soil; consequently, it is not clear if the larger gullies encompass more than one TFC.

Field observations indicate that TFCs crosscut most magmatic structures within the Cathedral Peak granodiorite (aplitic dikes, veins, megacrysts). The magmatic structures act as displacement markers, indicating exclusively opening-mode fracturing within TFCs. No shear offset is observed across any TFC or fracture within a TFC (Fig. 2b–e).

3.2. Microstructure

Thin sections of TFCs were observed using transmitted light and scanning electron microscopy (SEM). Large (>0.1 mm width) fractures are straight with slight undulations. These fractures are aligned sub-parallel to TFC boundaries, and are the fractures used to define TFC fracture density in the field (Fig. 5a). These large fractures crosscut all minerals and do not change orientation at grain boundaries. The fractures preferentially follow cleavage planes in potassium feldspar and biotite that are oriented sub-parallel to the fractures. Where fractures crosscut quartz grains, their orientation is more variable than within either feldspar or biotite grains. Only opening-mode displacement is observed along these fractures, as observed by offset grain contacts.

Large fractures locally contain micro-breccia consisting of angular fragments of feldspar, biotite, and quartz (Fig. 5a–d). The majority of clasts cannot be fit back into the fracture walls, although in some cases, clasts are clearly derived from adjacent minerals (Fig. 5b). Clasts of any composition are aligned sub-parallel to fracture walls and are situated in either void space, which is likely plucked material, or a fine-grained matrix (Fig. 5c). Electron dispersive spectroscopy (EDS) on the SEM indicates that the fine-grained matrix is dominantly zeolite with minor amounts of quartz. Accumulations of the zeolite are observable on the macro-scale (Fig. 4b), forming tabular regions up to 1.5 cm thick. This type of mineralization is observed in at least one TFC at each locality where TFCs are documented.

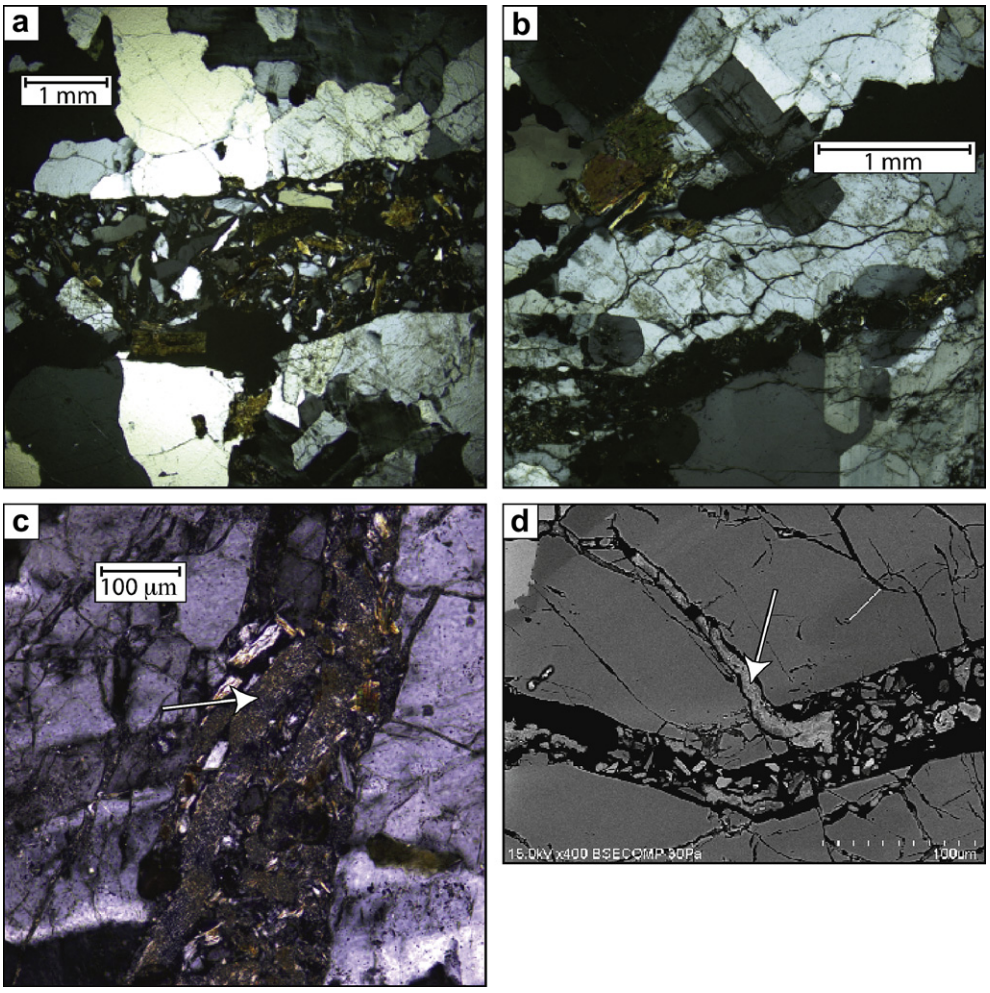

Fig. 5. a) Cross-polarized light photomicrograph of a large TFC fracture. Note the lack of shear offset recorded by grains on either side of the fracture, and the angular clasts within the fracture. b) Cross-polarized light photomicrograph of micro-fracturing (arrow) occurring at the tip of two larger fractures. At its tip, the large fracture is less planar, and the micro-fractures are highly irregular, forming branching patterns outside the large fractures. c) Cross-polarized light photomicrograph of a large fracture with zeolite/quartz assemblage and entrained angular clasts of host rock. d) SEM backscattered electron image of fracturing within a TFC, showing the zeolite/quartz assemblage (arrow) and micro-breccia.

Smaller transgranular and intragranular fractures are abundant within TFCs, regardless of grain composition. These smaller (<0.2 mm in width) fractures are concentrated near larger fracture tips, branching off the main fracture and forming dendritic patterns (Fig. 5b). The fractures are 1–5 mm in length, display large variations in orientation, and contain numerous bifurcations. This pattern results in grains that are heavily fractured near the tips of large fractures. Away from fracture tips, abundant micro-fracturing also exists in grains abutting large fracture walls. In these settings, the micro-fractures have preferential orientations that are sub-parallel and perpendicular to the large fractures.

Minor mineralization and alteration is observed along TFC fractures in thin section. Where small fractures crosscut biotite along cleavage planes, minor alteration to chlorite is observed. In addition to chlorite, whole biotite grains are also altered. To determine the mineralogy of the altered biotite, a TFC hand-sample was crushed and sieved to <250 μm. The crushed grains were examined under a reflective light microscope and altered biotite grains were plucked from the crushed ground mass. The altered grains are vermiculite, as determined by X-ray diffraction, which is orange in color. Consequently, we interpret the orange alteration rind observed at the macro-scale to be a product of significant biotite alteration to vermiculite.

4. Regional distribution

A systematic search for TFCs was conducted throughout the Tuolumne Intrusive Suite was conducted over the course of two field seasons. Field mapping of these structures indicates that TFCs are concentrated in the central portion of the Cathedral Peak granodiorite (Fig. 6). These features are best developed near the Johnson granite porphyry, where they are sub-vertical, and generally form in a single orientation (NNE-SSW). We note that previous workers (Mayo, 1941; Lockwood and Moore, 1979; Ericson et al., 2005) recognized the existence of this prominent NNE-SSW fracture system in this region. A second set of TFCs occurs where the NNE-SSW set has a spacing of <2 m. The second set of TFCs are oriented WNW-ESE, nearly orthogonal to the NNE trending set (Fig. 6). These 'orthogonal' TFCs are typically shorter than the NNE-striking TFCs. WNW-striking TFCs either terminate at a NNE-striking TFCs or terminate in the host rock; in Tuolumne Meadows, they typically do the former.

The only exception to these orientations is in the NE part of the Cathedral Peak granodiorite, where the pluton is affected by the CascadeLake shear zone (Fig. 6; Tikoff et al., 2005). Adjacent (~1 km) to the shear zone, some TFCs are oriented sub-parallel to the shear zone (NNW-SSE).

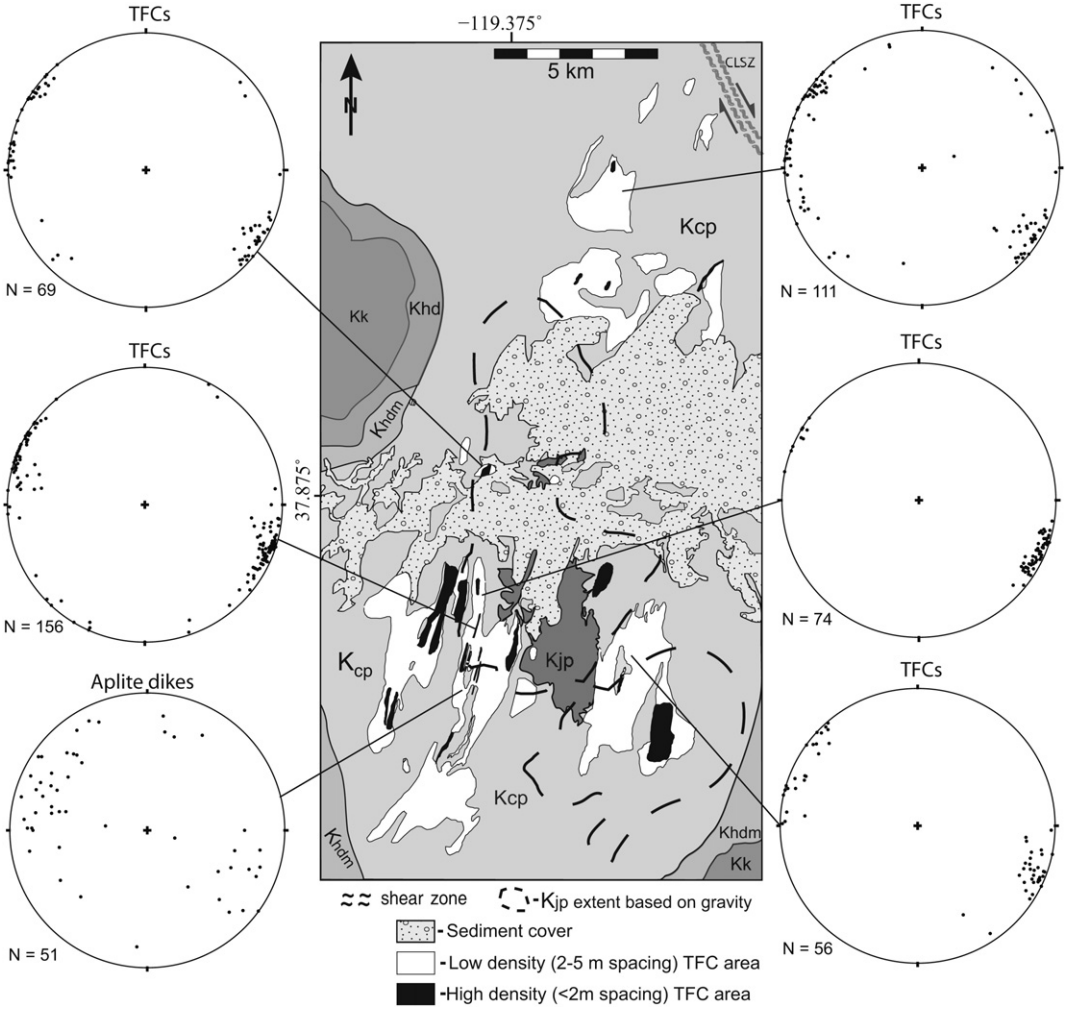

Fig. 6. Geologic map indicating extent of TFCs in the boxed region of Fig. 1, denoting regions of high and low TFC density. Sub-surface extent of the Johnson granite porphyry, as indicated by gravity surveys (Titus et al., 2005), is shown by dashed line. Abbreviations are those used in Fig. 1. Lower hemisphere equal-area nets are of poles to TFCs or aplite dikes (as labeled) from the designated locations.

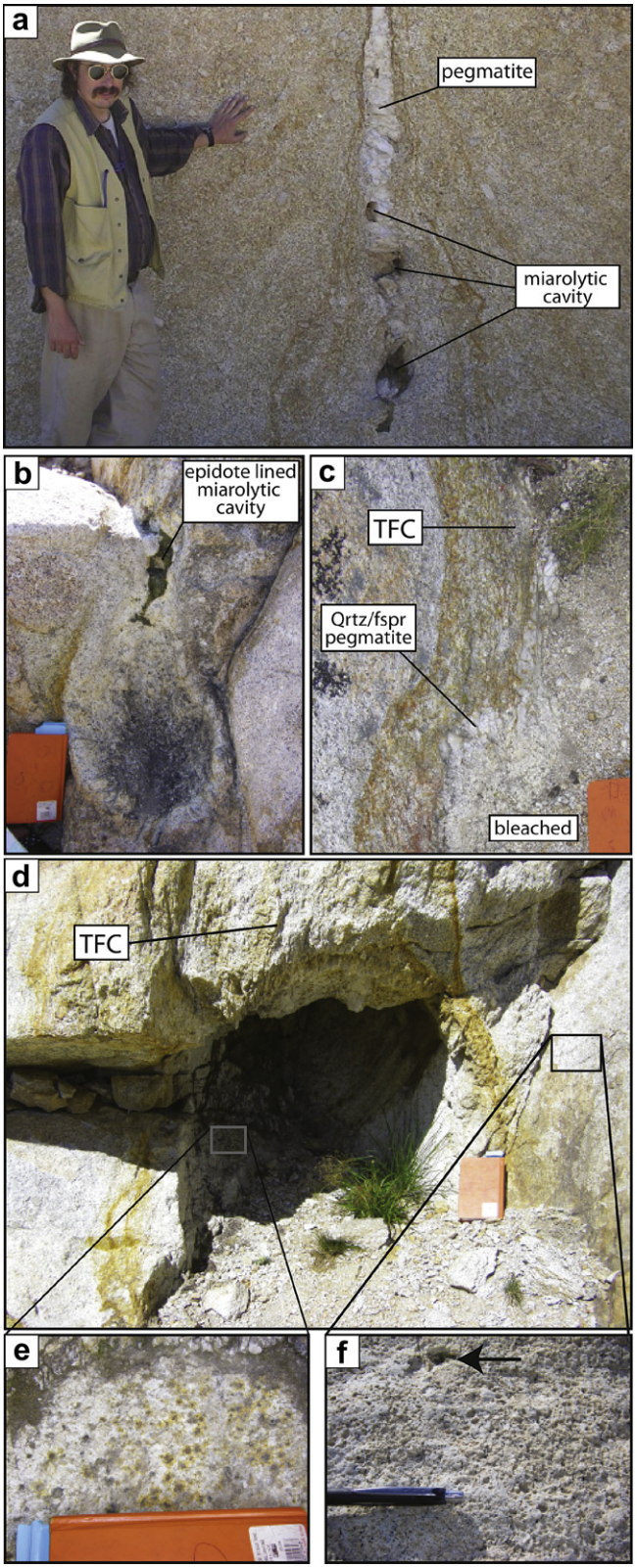

Fig. 7. a) Pegmatite dike and miarolitic cavity in the Cathedral Peak granodiorite. b) Field photograph of spherical structure near Matthes Crest. Note the bleached interior, spherical shape, and epidote lined miarolitic cavity emanating from one end of the sphere. c) TFC emanating from spherical structure near Lembert Dome, illustrating pegmatite lining the edges of the sphere, and the bleached interior. d) TFC emanating from a large spherical structure. Boxed areas show location of (e) and (f). e) Close-up of bleached interior of spherical structure, with iron stain surrounding mafic minerals. f) Cathedral Peak granodiorite next to spherical structure, displaying a 'pock-marked' weathering pattern that differs from weathering patterns elsewhere in the pluton. Arrow points to hole lined with epidote.

TFCs are not observed as isolated, individual features. Rather, swarms of TFCs occur throughout the Cathedral Peak granodiorite.Swarms of TFCs are termed 'high density' when found with spacing < 2m, and 'low density' when spacing ranges from 2 to 5 m, with spacing measured perpendicular to TFC strike. The swarms of TFCs occur along a NNE-WSW trending swath through the central portion of the Cathedral Peak pluton, with areas of high TFC density dominantly found near the Johnson granite porphyry (Fig. 6).

Fractures are present in plutons adjacent to the Cathedral Peak granodiorite (Half Dome granodiorite and Johnson granite porphyry), but we have not observed TFCs in these units. TFCs were locally observed crossing from the Cathedral Peak granodiorite contact into a single fracture as it continued into the Johnson granite porphyry. Where this transition occurs, the fracture in the Johnson granite porphyry retains the orientation of the TFC observed in the Cathedral Peak granodiorite (i.e., no apparent refraction of the structure across the contact).

5. Associated magmatic structures

The Cathedral Peak granodiorite is known for containing a variety of magmatic to sub-magmatic features (Bateman and Chappell, 1979; Bateman, 1992; Titus et al., 2005; Glazner et al., 2008; Paterson, 2009; Zák et al., 2009). Our field observations indicate that there is a close spatial association of TFCs with magmatic features. Given that the direct association of igneous magmatic features and a fracture system is unusual, we outline the relations below.

5.1. Pegmatite dikes, miarolitic cavities, and spherical alteration zones

Pegmatite dikes in the field area consist of quartz, potassium feldspar, plagioclase, biotite, tourmaline, and epidote, although all phases are not always present. Crystals within pegmatites range in size from ~5 cm up to ~15 cm, with quartz and potassium feldspar forming the largest crystals. These pegmatite dikes often contain miarolitic cavities, consisting of a 2–10 cm void space with euhedral crystals growing inward from the walls of the surrounding rock into the void (Fig. 7a). Miarolitic cavities consisting solely of inward-growing epidote crystals are observed in the pegmatite dikes, but more frequently contain quartz, potassium feldspar, plagioclase, and epidote crystals.

TFCs are observed in association with pegmatite dikes. Fig. 7a shows a pegmatite dike, with miarolitic cavities, that are surrounded by the orange alteration that envelopes most TFCs. Out of view in Fig. 7a is a TFC that strikes perpendicular to the pegmatite dike. Due to ground cover, it is not possible to observe the exact relationship at the pegmatite dike-TFC contact, but the orange alteration rind continuously envelopes both structures.

TFCs are also associated with another magmatic feature in the Cathedral Peak granodiorite, which we tentatively refer to as spherical alteration zones. The structures are spherical in shape, ranging in size from ~5 cm up to 150 cm in diameter, and consist of altered granodiorite (Fig. 7b). Within the zone, the granodiorite has been bleached (Fig. 7c–e), similar to the 'bleached zones' described for Mt. Abbot joints (cf. Segall et al., 1990). Within the bleached area, small (1–2 cm) red halos surround biotite crystals. Adjacent to the spherical alteration zones, the Cathedral Peak granodiorite displays a 'pock-marked' morphology consisting of small holes ranging in size from 0.5 to 2.0 cm (Fig. 7f). Field observations

suggest that the holes are where potassium feldspar crystals were once located. It is unclear whether the holes record preferential removal of potassium feldspar or removal of a potassium feldspar alteration product. In some instances the holes are lined with epidote, suggesting those holes existed in the presence of magmatic fluids (Fig. 7f). At the margins of the spherical alteration zones, pegmatite and miarolitic cavities are observed, containing potassium feldspar, quartz and plagioclase (Fig. 7b,c).

The spherical alteration zones are frequently observed in direct structural continuity with TFCs (Fig. 7c,d). There are two geometric arrangements observed: 1) Spherical alteration zones are the emanation point for TFCs (Fig. 7c,d); and 2) Spherical alteration zones occur along TFC margins. Where TFCs emanate from spherical alteration zones, they start as a wide zone of dense fracturing. This situation differs from more typical terminations of TFCs, which tip out along 1–2 fractures. In cases where spherical alteration zones occur along TFC margins, the alteration zones deviate from a spherical shape and are often hemispheres. Despite the association of TFCs with spherical alteration zones, no fracturing is observed in either their bleached interior or the pegmatitic margin.

5.2. Aplite dikes

Within the Cathedral Peak granodiorite, aplite dikes range in size from mm-to-m in width and m-to-100s of m in length. Dike abundance increases towards the contact with the Johnson granite porphyry. Aplite dike orientations collected near Matthes Lake range in dip from 40° to nearly vertical, and preferentially strike either NE or NW, similar to TFCs (Fig. 6). Despite the similarity in strike, aplite dikes do not transition to TFCs along strike. Where TFCs crosscut aplite dikes, the TFCs narrow and have lower fracture density in the dike than in the adjacent Cathedral Peak granodiorite. This observation indicates that the coarse-grained nature of the Cathedral Peak granodiorite is particularly conducive for the formation of the TFCs.

6. Strain analysis

South of the Tuolumne Intrusive Suite (Mt. Abbot area), the opening of extensional fractures has accommodated up to ~0.07% elongation (Segall and Pollard, 1983a), but these fractures occur more widely spaced than the fracturing associated with TFCs. Given the unique nature of TFCs as clustered sets of extensional fractures, we therefore provide estimates on the extensional strain accommodated by TFCs for comparison to the Mt. Abbot area fractures.

6.1. Methods

The total amount of elongation perpendicular to a series of parallel TFCs can be expressed as, *e*,

$$e = \frac{\sum \text{elongation}}{L_{\text{transect}} - \sum \text{elongation}} \quad (1)$$

Where L_{transect} is the length of the transect perpendicular to the average TFC strike and $\Sigma_{\text{extension}}$ is the sum of TFC extension values perpendicular to TFC strike. The elongation can be expressed as a stretch, *S*.

$$S = \frac{L_{\text{transect}} + \sum \text{elongation}}{L_{\text{transect}}} \quad (2)$$

Estimates of the elongation accommodated by TFCs were done at the locations shown in Fig. 8, using the data shown in Fig. 3 and Table 1. Using the recorded fracture densities in Fig. 3, the harmonic mean for all measured TFC fracture densities was 10.4 per 10 cm.

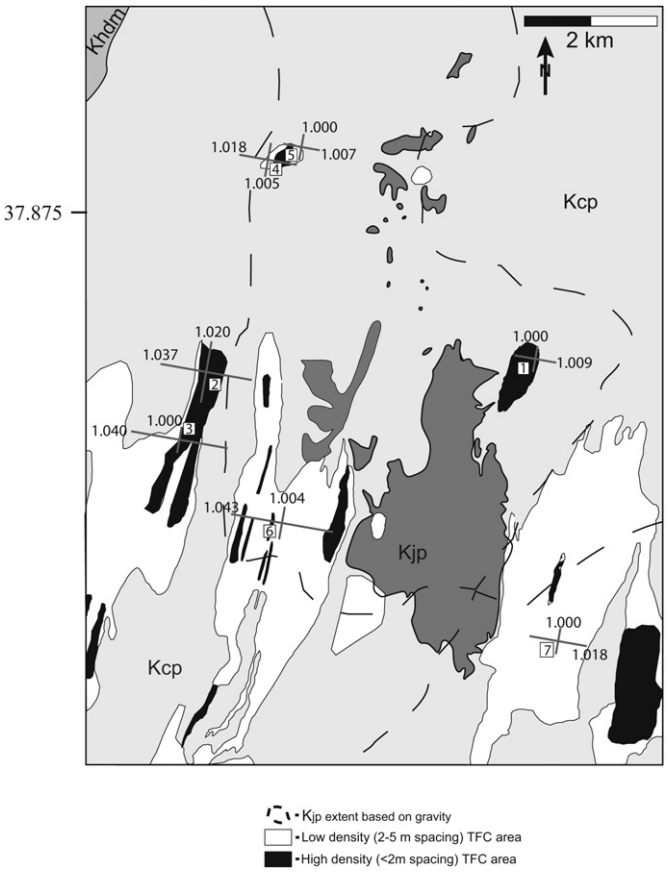

Fig. 8. Geologic map of the central field area showing extent of TFCs and TFC strain analysis at selected localities. Solid lines show magnitude and orientation of elongation, with the corresponding numbers indicating magnitude of stretch. Values were calculated from data presented in Table 1. Dashed line indicates sub-surface extent of the Johnson granite porphyry based on gravity (Titus et al., 2005).

Thin section observations indicate macro-scale fractures have apertures of ~0.10–0.15 cm (Fig. 5). Since further opening of the fractures during exhumation likely has occurred, we use a fracture aperture of 0.10 cm for our strain calculations.

Either one or two transects were measured, depending on whether only the NNE-striking set or the two orthogonal sets are present. A transect was measured perpendicular to each TFC orientation, measuring the transect distance (L_{transect}), the total number of TFCs, and the average TFC width, with each transect beginning and ending at a TFC. The amount of elongation

Table 1
Measurements and strain estimates from transects at the locations shown in Fig. 9.

Location	Transect orientation	# of TFCs Measured	Transect Length (m)	Average Spacing (m)	Average Width (m)	% Elongation
1	100	7	20.4	1.45	0.24	0.9
2	100	5	4.7	0.70	0.34	3.9
2	010	12	17.3	1.30	0.28	2.1
3	100	9	20.2	0.90	1.37	4.2
4	100	8	22.0	2.21	0.49	1.9
4	010	8	24.1	3.06	0.20	0.7
5	100	8	24.0	2.12	0.14	0.5
6	100	8	35.0	2.29	1.83	4.5
6	010	11	84.0	5.50	0.40	0.4
7	100	11	44.0	3.90	0.69	1.8

accommodated by the opening of fractures in an average TFC (e_{avg}) was determined using the estimates on fracture density, fracture aperture, and average TFC width. The total number of TFCs along a given transect was then multiplied by e_{avg} to determine $\Sigma_{elongation}$. Finally, the stretch in the direction of the transect was calculated using (2). For field sites with both sets of TFCs, a stretch is thus calculated in two orthogonal directions.

Due to the dominance of the NNE-striking TFCs in the field area, the direction orthogonal to the NNE-striking TFC set is the maximum principal strain axis (S_1), and the direction orthogonal to the secondary, WNW-striking set is the intermediate principal strain axis (S_2). There is no evidence for elongation or shortening in the vertical direction, hence $S_3 = 1$.

6.2. Results

The results of the strain analysis are shown as stretches in the S_1–S_2 plane in the area around Tuolumne Meadows (Fig. 8). The solid lines illustrate the orientation of S_1 and S_2 with the corresponding numbers indicating the magnitude of stretch. For the seven transects of NNE-striking TFCs, stretches range from 1.005 to 1.043 (unitless), or from 0.5 to 4.5 percent elongation, and trend in the direction of 100. For the three transects of WNW-striking TFCS, stretches range from 1.004 to 1.020, or from 0.4 to 2.1 percent elongation, and have a trend of 010. Where the WNW-striking TFC set is absent, we assume no elongation perpendicular to strike ($S_2 = S_3 = 1$).

The largest elongation occurs to the west of the Johnson granite porphyry, south of Tuolumne Meadows (locations 2, 3, 7). At these field sites, elongation in the WNW direction is as high as 4.5%. On the east side of the Johnson granite porphyry (locations 1, 8) and in Tuolumne Meadows (locations 4, 5) elongation in the WNW direction is lower than 2%. In the NNE direction, the percent elongation is largest in the vicinity of the largest WNW elongations. At every field location, the NNE-elongation is lower than the WNW-elongation.

7. Discussion

7.1. Fracturing in the Sierra Nevada Batholith

TFCs are structurally different from previously described Sierra Nevada Batholith fracture sets. Other fracture sets in the Sierra Nevada Batholith are interpreted to result from: 1) thermal contraction (Bergbauer and Martel, 1999); 2) Sheeting or exfoliation (Jahns, 1943; Martel, 2006); 3) directional compressive stress (Martel and Pollard, 1989; Christiansen and Pollard, 1995); or 4) reactivation of joints as strike-slip faults (e.g., Segall and Pollard, 1983a,b; Pachell and Evans, 2002). Given that the TFCs are structurally related to magmatic features (Fig. 7), we interpret them to be Cretaceous features that formed when the magmatic arc was active. Given that other large-scale systematic fracture sets formed in the Late Cretaceous and have been extensively documented in the Mt. Abbot quadrangle (Lockwood and Lydon, 1975; Lockwood and Moore, 1979; Segall et al., 1990), we provide a comparison of TFCs to the Mt. Abbot fracture sets.

TFCs and the Mt. Abbot fracture set have similar orientations (steeply dipping, NE-SW strike) and both occur in granitic rock of a similar age (~90–80 Ma). Despite these similarities, several key differences exist. First, the diagnostic characteristic of a TFC is extraordinarily high fracture density (>4 per 10 cm). In the Mt. Abbot area, fracture density is ≤0.5 per 10 cm (Segall and Pollard, 1983a). Fracture densities in TFCs can reach 18 per 10 cm, more than an order of magnitude higher than those observed in the southern batholith. Next, there is no evidence for microscopic or macroscopic shear offset along TFCs, regardless of orientation or location. Joints, shear fractures, and strike-slip faults in the Mt. Abbot area are interpreted to have originated as joints, with some joint orientations reactivating to form shear fractures (Segall and Pollard, 1983b; Segall and Simpson, 1986). If a similarity between the two fracture systems (TFCs vs. Mt. Abbot) existed, we would expect shear offset along TFCs similarly oriented to Mt. Abbot shear fractures.

Mineralization is observed along fractures in both settings, but differs in character. TFCs have an orange color due to the alteration of bioitite to vermiculite. Conversely, joints and shear fractures in the Mt. Abbot area are commonly associated with a 'bleached zone' (Segall and Pollard, 1983a; Segall et al., 1990). Also, the only macroscopic mineralization within TFCs is zeolite, whereas an extensive amount of epidote is observed along other documented Sierra Nevada extensional fractures (Segall and Pollard, 1983a, 1983b; Segall et al., 1990).

The microstructure of TFC fractures also differs from the Mt. Abbot joints. Joints in the Mt. Abbot area are characterized by a single mineralized fracture containing epidote, zeolite, and white mica (Segall and Pollard, 1983a; Segall et al., 1990). TFC fractures demonstrate a complex character consisting of sub-planar large fractures filled with micro-breccia, and dendritic micro-fracturing patterns at the large fracture tips.

We contend that TFCs are clearly different from previously described fracture systems in the Sierra Nevada Batholith. TFCs, however, are unlikely to be unique to the Cathedral Peak granodiorite. TFCs are exposed in the glaciated High Sierra Nevada because of the superb exposure. In similar geologic settings with limited exposure, TFCs could be present, but easily overlooked due to erosion.

7.2. Doming above the Johnson granite porphyry

The orientation of Cretaceous fracture sets in the Mt. Abbot area is interpreted to result from the direction of maximum horizontal tectonic stress (Martel and Pollard, 1989; Christiansen and Pollard, 1995) and thermal contraction (Bergbauer and Martel, 1999). However, several key differences indicate that TFC orientations are controlled by other processes. First, there is regional development of a WNW-striking TFC set, an orientation not extensively present in the Mt. Abbot area. Second, the percent elongation recorded by TFCs (0.4–4.5) is over an order of magnitude higher than values recorded by joints in the Mt. Abbot area (Segall and Pollard, 1983a). Finally, the two dominant strikes of TFCs (NNE and ESE) record extension sub-parallel and sub-perpendicular to the long axis of the Johnson granite porphyry. These observations suggest an alternative mechanism may have influenced the observed pattern of TFCs.

We suggest that the pattern of TFCs is controlled by doming above the intruding Johnson granite porphyry, based on the observed spatial relations. TFCs are best developed in proximity to the exposed and sub-surface extent of the Johnson granite porphyry (Fig. 6). Furthermore, the NNE-striking TFC orientation - that records the maximum elongation - strikes parallel to the long axis of the intrusion (Fig. 8). The two orientations of TFCs occur only adjacent to the exposure of the Johnson granite porphyry, which presumably has the most doming. Similar patterns are observed above other igneous intrusions. Doming can produce extension fractures above resurgent igneous bodies (e.g., Gudmundsson, 1998; Acocella, 2010), and has been shown experimentally (Cloos, 1955). Surrounding magmatic intrusions, the pattern of extension fractures is commonly manifested as two orthogonal sets, with one set radial and the other concentric to the crest of the dome (Koide and Bhattacharji, 1975). Therefore, the simplest explanation for the

observed patterns is that the TFCs formed in response to uplift associated with magmatic intrusion.

7.3. Tabular fracture cluster formation

7.3.1. Presence of volatiles

TFCs likely formed in the presence of significant volatile pressures, as supported by the spatial association with fluid-rich magmatic features (Figs. 7 and 9). The Cathedral Peak granodiorite is known to have a range of magmatic structures, such as tubes, troughs, and small pipes (Paterson, 2009). The presence of miarolitic cavities – indicative of high (~300 MPa) fluid pressure (Candela, 1997) – with TFCs, suggests pockets of volatiles existed where TFCs formed. We interpret the spherical alteration zones in the same manner as miarolitic cavities; localities where volatiles were once concentrated. The spherical alteration zones display a bleached interior; this bleaching is interpreted elsewhere in the Sierra Nevada Batholith to be a product of hydrothermal alteration (cf. Segall and Pollard, 1983a; Segall et al., 1990). Pegmatitic material lining the margins of the spherical alteration zones indicates abundant fluids near the alteration zones.

The composition of material within the TFCs also supports the interpretation of localized volatile concentration. The fine-grained quartz and zeolite - interpreted to be hydrothermally altered feldspar as observed in other settings (Galli and Passaglia, 1973; Svenson et al., 2006) - suggests minor amounts of melt intruded the fractures. The presence of zeolite and vermiculite along TFCs, both absent in the adjacent host rock, suggests subsequent hydrothermal exploitation of TFCs.

There are two possible sources for the volatiles: the Cretaceous Johnson granite porphyry or the Miocene magmatism in the area (specifically, Little Devil's Postpile). TFCs occur in the highest density in close proximity to exposed Johnson granite porphyry, or where sub-surface Johnson granite porphyry is interpreted to be located based on gravity (Titus et al., 2005) (Fig. 6). In addition, the Johnson granite porphyry is interpreted to have been fluid rich and undergone rapid decompression and quenching (Bateman, 1992; Titus et al., 2005), and thus could feasibly produce pockets of volatile overpressure. Alternatively, the other viable source of volatiles for TFC formation is the abundant Miocene magmatism to the north of the Tuolumne Intrusive Suite (Busby et al., 2008).

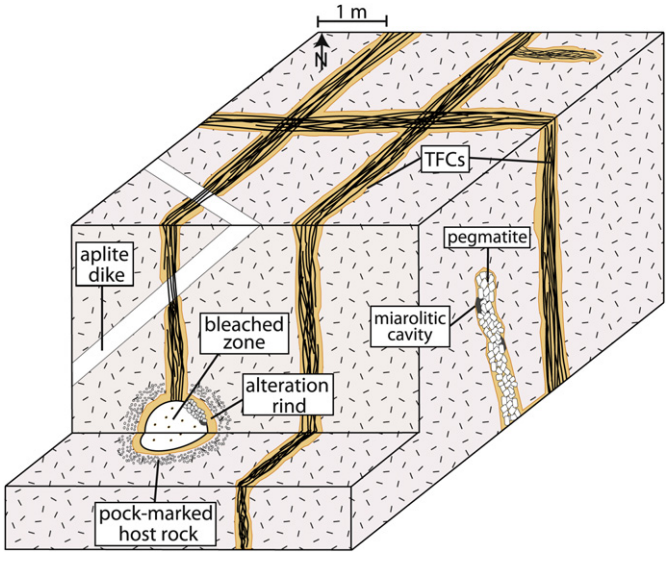

Fig. 9. Schematic block diagram indicating the key structural relations observed in this study.

Within the Cathedral Peak granodiorite, Miocene volcanism is only observed at Little Devil's Postpile – a stack of columnar jointed basalt - in the west-central portion of the Cathedral Peak granodiorite. TFCs do exist in this vicinity, although not in the abundance observed near the Johnson granite porphyry.

We strongly favor the hypothesis that the Johnson granite porphyry was the source of volatile overpressure for the reasons that follow. First, TFCs are rare to absent in the northwestern portion of the Cathedral Peak granodiorite (i.e., in areas furthest from the Johnson granite porphyry) (Fig. 6). Second, aside from the TFCs observed near the CascadeLake shear zone, all TFCs are found within 5 km of exposed Johnson granite porphyry. In addition, the highest densities of TFCs are found within 2 km of the Johnson granite porphyry (Fig. 6). Finally, the dominant TFC orientation (NNE–SSW) is parallel to the overall trend of the Johnson granite porphyry, and the strain pattern is consistent with doming related to the Johnson granite porphyry (Fig. 8). There is no such spatial link of TFCs with Miocene magmatism, which is more prevalent to the north of the Cathedral Peak granodiorite where TFCs are absent. Based on these observations, we interpret the Johnson granite porphyry as the fluid source.

7.3.2. Fracturing associated with volatile overpressure

There is a clear spatial association of TFCs, magmatic features indicating the presence of volatiles, and the location Johnson granite porphyry. The question remains: to what extent did high volatile pressures contributed to the unique fracturing style of the TFCs? In thermally-driven models of stratified magma chambers consisting of bubble rich and bubble-poor layers, bubble rich layers will eventually concentrate at the top of the magma chamber due to Rayleigh-Taylor instabilities (Ruprecht et al., 2008). A volatile-rich pluton such as the Johnson granite porphyry could thus be expected to develop volatile-rich layers near its top. Simulations of the movement of bubble rich magma (i.e., volatile-rich) through a magma chamber suggest that bubble rich magma will localize and form conduits to permit its upward movement (Ruprecht et al., 2008).

The spatial association of magmatic structures and TFCs, listed above, are consistent with interpretation of TFCs forming due to volatile overpressure. In particular, the TFCs emanating as fully developed zones from spherical alteration zones is strongly suggestive of a causal relationship between volatiles and densely spaced fracturing. Furthermore, volatile overpressure is known to lead to tensile fracturing in magmatic settings, whether due to replenishment (Blake, 1981) or volatile saturation of melt due to crystallization (Burnham, 1979; Blake, 1984). The ubiquitous micro-brecciation observed in the TFCs requires a magmatic volatile source for the mineralization, and the same volatile source is likely the cause of the dense fracture formation. The rapid release of volatiles, as documented for phreatic eruptions (Svenson et al., 2006; Brown et al., 2007), can thus occur through structures such as TFCs.

We envision the following scenario for TFC development. As fluid pressure increased within local pockets in the Cathedral Peak granodiorite, it became overpressured. Once the fluid pressure overcame the lithostatic load, the volatiles were explosively released through the formation of TFCs, causing micro-brecciation of the host rock. Accompanying the volatile release was the minor intrusion of melt along the fractures. Once the TFCs were formed, they became fluid pathways in an otherwise impermeable rock, resulting in concentrated hydrothermal alteration.

7.3.3. Dynamic fracturing

Linear elastic fracture mechanics has been used to explain other Sierra Nevada fracture sets (Segall and Pollard, 1980, 1983a, 1983b;

Pollard and Segall, 1987). However, the theory used in these studies predicts anti-clustered extension fractures. The opening of an extension fracture causes stress reduction in its immediate vicinity (stress reduction shadow), and should inhibit nearby formation of similarly oriented extension fractures (Hobbs, 1967; Pollard and Segall, 1987; Gross, 1993; Becker and Gross, 1996). Consequently, this does not fully explain the closely spaced extension fractures observed in TFCs.

Dynamic fracture mechanics provides an alternative set of conditions for fracture formation that may explain the high fracture densities observed in TFCs. Dynamic fracture mechanics refers to fracturing processes in which material inertia becomes important, whether through rapid loading or rapid crack propagation (Freund, 1990). During rapid fracture propagation, a single fracture propagating through a material is unstable, and the result is that the fracture bifurcates into numerous fractures (Grady and Kipp, 1987; Freund, 1990; Sagy et al., 2001, 2006). During rapid loading, a material does not have time to focus internal stresses on relatively few flaws causing more flaws to propagate fractures than during slow loading (Grady and Kipp, 1987). Thus, dynamic fracture mechanics permits zones of dense fracturing, and has been shown theoretically (Grady and Kipp, 1987; Freund, 1990) and experimentally (Sagy et al., 2001).

Within TFCs, bifurcations are observed on the micro-scale at fracture tips and fracture densities are elevated above densities observed in other extensional fracture sets in the Sierra Nevada Batholith (e.g., Segall and Pollard, 1983a). These observations are consistent with dynamic fracture experiments (Sagy et al., 2001). Assuming that TFCs result from the expulsion of volatiles from the Johnson granite porphyry through the Cathedral Peak granodiorite, dynamic fracture mechanics provides the theoretical explanation for the observed high fracture density. Volatile overpressure released in high energy, explosive events could cause fractures to propagate at unstable rates, causing the formation of clustered sets of extension fractures. Future modeling, either experimental or numerical, could elucidate the conditions necessary (rigidity of overlying layer, degree of overpressure, stress boundary conditions, etc.) for this to occur.

8. Conclusions

We present documentation of a previously undocumented type of fracture system – Tabular Fracture Clusters (TFCs) – present in the central section of the Cathedral Peak granodiorite, Sierra Nevada Batholith. TFCs are tabular zones of densely spaced, subparallel extension fractures that occur within the Cathedral Peak granodiorite, Sierra Nevada Batholith. Strain estimates indicate ENE–WSW elongation and locally an additional component of NNW–SSE elongation, consistent with deformation resulting from doming above the Johnson granite porphyry. The association with miarolitic cavities, nature of the fractures (opening-mode displacement, micro-breccia), dense spacing, and spatial association with the Johnson granite porphyry are consistent with the formation of TFCs concurrent with volatile expulsion from the Johnson granite porphyry.

We propose a conceptual TFC formation model in which rapid volatile expulsion led to dynamic fracturing. First, volatile overpressure developed within the Cathedral Peak granodiorite, with subsequent release of volatiles resulting in rapid fracture propagation. Initial tensile fractures propagated at unstable rates, and bifurcated into linear, dense fracture arrays. The resulting TFC spacing on a regional scale is based on the distribution of volatile overpressure, whereas fracture density within TFCs resulted from high strain rates due to volatile release.

Acknowledgements

This work was supported by a GSA graduate student grant and an AAPG grant-in-aid. PRR and BT thank M. Dyson, T. Kruckas, and J. Pesicek for help in the field. Constructive reviews/conversations from S. Woijtal and G. Stock improved this paper.

References

Acocella, V., 2010. Evaluating fracture patterns within a resurgent caldera: Campi Flegrei, Italy. Bulletin of Volcanology. doi:10.1007/s00445-010-0347-x.
Ague, J.J., Brimhall, G.H., 1988. Magmatic arc asymmetry and distribution of anomalous plutonic belts in the Batholiths of California: effects of assimilation, crustal thickness, and depth of crystallization. Geological Society of America Bulletin 100, 912–927.
Bateman, P.C., 1992. Plutonism in the central part of the Sierra Nevada Batholith, California. U.S. Geological Survey Professional Paper 1483, p. 186.
Bateman, P.C., Chappell, B.W., 1979. Crystallization, fractionation, and solidification of the Tuolumne intrusive series, Yosemite National Park, California. Geological Society of America Bulletin 90, 465–482.
Becker, A., Gross, M.R., 1996. Mechanism for joint saturation in mechanically layered rocks: an example from southern Israel. Tectonophysics 257, 223–237.
Bergbauer, S., Martel, S.J., 1999. Formation of joints in cooling plutons. Journal of Structural Geology 21, 821–835.
Blake, S., 1981. Volcanism and the dynamics of open magma chambers. Nature 289, 783–785.
Blake, S., 1984. Volatile oversaturation during the evolution of silicic magma chambers as an eruption trigger. Journal of Geophysical Research 89, 8237–8244.
Brown, R.J., Kavanagh, J., Sparks, R.S.J., Tait, M., Field, M., 2007. Mechanically disrupted and chemically weakened zones in segmented dike systems cause vent localization: evidence from kimberlite volcanic systems. Geology 35, 815–818. doi:10.1130/G23670A.1.
Burnham, C.W., 1979. The importance of volatile constituents. In: Yoder, H.S. (Ed.), The Evolution of Igneous Rocks. PrincetonUniversity Press, pp. 439–482.
Busby, C.J., DeOreao, S.B., Skilling, I., Gans, P.B., Hagan, J.C., 2008. Carson Pass – Kirkwood paleocanyon system: Paleogeography of the ancestral Cascades arc and implications for landscape evolution of the Sierra Nevada (California). Geological Society of America Bulletin 120, 274–299. doi:10.1130/B25849.1.
Candela, P.A., 1997. A review of shallow, ore-related granites: textures, volatiles and ore metals. Journal of Petrology 38, 1619–1633.
Christiansen, P.P., Pollard, D.D., 1995. Nucleation growth and structural development of mylonitic shear zones in granitic rocks. Journal of Structural Geology 19, 1159–1172.
Cloos, E., 1955. Experimental analysis of fracture patterns. Geological Society of America Bulletin 66, 241–256.
Coleman, D.S., Glazner, A.F., 1997. The Sierra Crest magmatic event: rapid formation of juvenile crust during the Late Cretaceous in California. International Geology Review 39, 768–787.
Coleman, D.S., Gray, W., Glazner, A.F., 2004. Rethinking the emplacement and evolution of zoned plutons: Geochronologic evidence for incremental assembly of the Tuolumne Intrusive Suite, California. Geology 32, 433–436.
Cruikshank, K.M., Aydin, A., 1995. Unweaving the joints in Entrada sandstone, Arches National Park, Utah, USA. Journal of Structural Geology 17, 409–421.
d'Alessio, M., Martel, S.J., 2005. Development of strike-slip faults from dikes, Sequoia National Park, California. Journal of Structural Geology 27, 35–49.
Di Toro, G., Nielsen, S., Pennacchioni, G., 2005. Earthquake rupture dynamics frozen in exhumed ancient faults. Nature 436, 1009–1012. doi:10.1038/nature03910.
Ericson, K., Migon, P., Olvmo, M., 2005. Fractures and drainage in the granite mountainous area: a study from Sierra Nevada, USA. Geomorphology 64, 97–116.
Freund, L.B., 1990. Dynamic Fracture Mechanics. Cambridge University Press, Cambridge, 563 pp.
Galli, E., Passaglia, E., 1973. Stellerite from Villanova Monteleone, Sardinia. Lithos 6, 83–90.
Glazner, A.F., Coleman, D.S., Bartley, J.M., 2008. The tenuous connection between high-silica rhyolites and granodiorite plutons. Geology 36, 133–136.
Grady, D.E., Kipp, M.E., 1987. Dynamic rock fragmentation. In: Atkinson, B.K. (Ed.), Fracture Mechanics of Rock. Academic Press, London, pp. 429–475.
Greene, D.C., Schweickert, R.A., 1995. The Gem Lake shear zone: cretaceous dextral transpression in the northern Ritter range pendant, eastern Sierra Nevada, California. Tectonics 14, 945–961.
Griffith, W.A., Rosakis, A., Pollard, D.D., Ko, C.W., 2009. Dynamic rupture experiments elucidate tensile crack development during propagating earthquake ruptures. Geology 37, 795–798. doi:10.1130/G30064A.
Gross, M.R., 1993. The origin and spacing of cross-joints: examples from the Monterey Formation, Santa Barbara, California. Journal of Structural Geology 15, 737–751.
Gudmundsson, A., 1998. Formation and development of normal-fault calderas and the initiation of large explosive eruptions. Bulletin of Volcanology 60, 160–170.
Hobbs, D.W., 1967. The formation of tension joints in sedimentary rock: an explanation. Geology Magazine 104, 550–556.

Jahns, R.H., 1943. Sheet structure in granites: its origin and use as a measure of glacial erosion in New England. The Journal of Geology 51, 71–98.
Koide, H., Bhattacharji, S., 1975. Formation of fractures around magmatic intrusions and their role in ore localization. Economic Geology 70, 781–799.
Little, T.A., 1996. Faulting-related displacement gradients and strain adjacent to the Awatere strike-slip fault in New Zealand. Journal of Structural Geology 18, 321–340.
Lockwood, J.P., Lydon, P.A., 1975. Geologic map of the Mount Abbot quadrangle, Sierra Nevada, California. U.S. Geological Survey Geologic Quadrangle Map GQ-1155.
Lockwood, J.P., Moore, J.G., 1979. Regional deformation of the Sierra Nevada, California, on conjugate microfault sets. Journal of Geophysical Research 84, 6041–6049.
Martel, S.J., Pollard, D.D., 1989. Mechanics of slip and fracture along small faults and simple strike- slip fault zones in granitic rocks. Journal of Geophysical Research 94, 9417–9428.
Martel, S.J., 2006. Effect of topographic curvature on near-surface stresses and application to sheeting joints. Geophysical Research Letters 33, L01308. doi:10.1029/2005GL024710.
Mayo, E.B., 1941. Deformation in the interval Mount Lyell-Mount Whitney, California. Geological Society of America Bulletin 52, 1001–1084.
McNulty, B.A., 1995. Shear zone development during magmatic arc construction: the Bench Canyon shear zone, central Sierra Nevada, California. Geological Society of America Bulletin 108, 926–940.
Mitra, G., 1984. Brittle to ductile transition due to large strains along the white rock Thrust, Wind River Mountains, Wyoming. Journal of Structural Geology 6, 51–61.
Myers, R., Aydin, A., 2004. The evolution of faults formed by shearing across joint zones in sandstone. Journal of Structural Geology 26, 947–966.
Pachell, M.A., Evans, J.P., 2002. Growth, linkage, and termination processes of a 10-km-long strike-slip fault in jointed granite: the Gemini fault zone, Sierra Nevada, California. Journal of Structural Geology 24, 1903–1924.
Pachell, M.A., Evans, J.P., Lansing Tayler, W., 2003. Kilometer-scale kinking of crystalline rocks in a transpressive convergent setting, Central Sierra Nevada, California. Geological Society of America Bulletin 115, 817–831.
Paterson, S.R., 2009. Magmatic tubes, pipes, troughs, diapirs, and plumes: late-stage convective instabilities resulting in compositional diversity and permeable networks in crystal-rich magmas of the Tuolumne batholith, Sierra Nevada, California. Geosphere 5, 496–527. doi:10.1130/GES00214.1.
Pollard, D.D., Segall, P., 1987. Theoretical displacements and stresses near fractures in rock: With applications to faults, joints, veins, dikes, and solution surfaces. In: Atkinson, B.K. (Ed.), Fracture Mechanics of Rock. Academic Press, London, pp. 277–349.
Price, N.J., 1966. Fault and Joint Development in Brittle and Semi-brittle Rock. Pergamon Press, Oxford, 176 pp.
Ruprecht, P., Bergantz, G.W., Dufek, J., 2008. Modeling of gas-driven magmatic overturn. Tracking of phenocryst dispersal and gathering during magma mixing. Geochemistry Geophysics Geosystems 9, Q07017. doi:10.1029/2008GC002022.
Sagy, A., Reches, Z., Roman, I., 2001. Dynamic fracturing: field and experimental observations. Journal of Structural Geology 23, 1223–1239.
Sagy, A., Reches, Z., Fineberg, J., 2002. Dynamic fracture by large extraterrestrial impacts as the origin of shatter cones. Nature 418, 310–313.
Sagy, A., Fineberg, J., Reches, Z., 2004. Shatter cones: Branched, rapid fractures formed by shock impact. Journal of Geophysical Research 109, B10209. doi:10.1029/2004JB003016.
Sagy, A., Cohen, G., Reches, Z., Fineberg, J., 2006. Dynamic fracture of granular material under quasi-static loading. Journal of Geophysical Research 111, B04406. doi:10.1029/2005JB003948.
Segall, P., Pollard, D.D., 1980. Mechanics of discontinuous faults. Journal of Geophysical Research 85, 4337–4350.
Segall, P., Pollard, D.D., 1983a. Joint formation in granitic rock of the Sierra Nevada. Geological Society of America Bulletin 94, 563–575.
Segall, P., Pollard, D.D., 1983b. Nucleation and growth of strike-slip faults in granite. Journal of Geophysical Research 88, 555–568.
Segall, P., Simpson, C., 1986. Nucleation of ductile shear zones on dilatant fractures. Geology 14, 56–59.
Segall, P., McKee, E.H., Martel, S.J., Turrin, B.D., 1990. Late Cretaceous age of fractures in the Sierra Nevada batholith. Geology 18, 1248–1251.
Sharon, E., Fineberg, J., 1996. Microbranching instability and the dynamic fracture of brittle materials. Physical Review B 54, 7128–7139.
Svenson, H., Jamtveit, B., Planke, S., Chevallier, L., 2006. Structure and evolution of hydrothermal vent complexes in the Karoo Basin, South Africa. Journal of the Geological Society, London 163, 671–682.
Tikoff, B., de Saint Blanquat, M., 1997. Transpressional shearing and strike-slip partitioning in the Late Cretaceous Sierra Nevada magmatic arc, California. Tectonics 16, 442–459.
Tikoff, B., Davis, M.R., Teyssier, C., St. Blanquat, M., Habert, G., Morgan, S., 2005. Fabric studies within the Cascade Lake shear zone, Sierra Nevada, California. Tectonophysics 400, 209–226.
Titus, S.J., Clark, R., Tikoff, B., 2005. Geologic and geophysical investigation of two fine-grained granites, Sierra Nevada Batholith, California. Evidence for structural controls on emplacement and volcanism. Geological Society of America Bulletin 117, 1256–1271.
Watterson, J., Walsh, J.J., Gillespie, P.A., Easton, S., 1996. Scaling systematics of fault sizes on a large-scale range fault map. Journal of Structural Geology 18, 199–214.
Zák, J., Paterson, S.R., Kabele, P., Janoušek, V., 2009. The Mammoth Peak sheeted complex, Tuolumne batholith, Sierra Nevada, California: a record of initial growth or late thermal contraction in a magma chamber? Contributions to Mineralogy and Petrology 158, 447–470.